

December 2023

An Ensemble DNN Model for Automatic Detection of COVID-19 from CXR Scans

Hagar Hesham Eldawoudy

Electronics and Communications Engineering Department, Faculty of Engineering, Mansoura University, Mansoura 35516, Egypt, hagerhesham653@gmail.com

Mohamed Abdelazim Mohamed

Electronics and Communications Engineering Department, Faculty of Engineering, Mansoura University, Mansoura 35516, Egypt

Eman AbdElhalim

Electronics and Communications Engineering Department, Faculty of Engineering, Mansoura University, Mansoura 35516, Egypt

Follow this and additional works at: <https://mej.researchcommons.org/home>



Part of the [Architecture Commons](#), and the [Engineering Commons](#)

Recommended Citation

Eldawoudy, Hagar Hesham; Mohamed, Mohamed Abdelazim; and AbdElhalim, Eman (2023) "An Ensemble DNN Model for Automatic Detection of COVID-19 from CXR Scans," *Mansoura Engineering Journal*: Vol. 49 : Iss. 1 , Article 10.

Available at: <https://doi.org/10.58491/2735-4202.3116>

This Original Study is brought to you for free and open access by Mansoura Engineering Journal. It has been accepted for inclusion in Mansoura Engineering Journal by an authorized editor of Mansoura Engineering Journal. For more information, please contact mej@mans.edu.eg.

ORIGINAL STUDY

An Ensemble DNN Model for Automatic Detection of COVID-19 from CXR Scans

Hagar H. Eldawoudy ^{a,*}, Mohamed A. Mohamed ^b, Eman Abdelhalim ^b

^a Department of Electronics and Communications Engineering, Mansoura Higher Institute for Engineering and Technology, Egypt

^b Electronics and Communications Engineering Department, Faculty of Engineering, Mansoura University, Mansoura 35516, Egypt

Abstract

The new coronavirus 2019 (COVID-19) pandemic has been destructive to human life and has resulted in a significant number of deaths globally. Detecting COVID-19 as early as possible is a critical way to prohibit the virus from quickly passing among people. RT-PCR is a method used for COVID-19 detection, but it is very expensive and is not an accurate method due to its sensitivity of 60–70%. For these reasons, deep learning and imaging techniques are combined by doctors, scientific experts, and professionals for accurate and rapid COVID-19 detection. In this work, we propose a stacked ensemble model based on linear regression for automatic COVID-19 detection on the chest using radiographic scans based on the techniques of deep learning. The suggested model concept is based on fusing the features of the three pretrained models, namely ResNet-152, DenseNet-201, and Vgg-19, and its performance is higher than using single models. We collected a balanced dataset from various repositories on the 'Kaggle' website and split it into training and testing sets. Our proposed model was tested on 11100 COVID-19, normal, and pneumonia images. Also, we used different optimizers for evaluations, such as Adam, Adagrad, ASGD, and SGD optimizers, using six epochs for the training process and a learning rate of 0.01. Using the SGD optimizer with our proposed model achieved the highest prediction accuracy, recall, precision, F1-score, and AUC for 3-class classification among other optimizers.

Keywords: Artificial intelligence (AI), Artificial neural networks (ANNs), Chest X-ray (CXR), Deep learning (DL), Ensemble model (EM), Linear regression (LR), Transfer learning (TL), Deep neural Network (DNN)

1. Introduction

In December 2019, the coronavirus disease became a highly infectious illness that threatened human life. It was spread between humans through direct or indirect contact with infected people and has already spread over the world. COVID-19 is a contagious virus caused by the new coronavirus called severe acute respiratory syndrome coronavirus 2 (SARS-CoV-2). Coronavirus symptoms may include fever, coughing, changes in or loss of taste and smell, and shortness of breath. SARS-CoV-2 has some similarities with SARS-CoV and MERS-CoV because they belong to the same family. Severe acute respiratory syndrome (SARS-COV) and (MERS-COV) are called Middle East respiratory

syndromes, which both affect the human respiratory system (Narin et al., 2021). According to the World Health Organization [WHO] reports, COVID-19 was considered a pandemic in January 2020. Also, according to its latest records, in April 2023, more than 762 million people worldwide had been afflicted by the coronavirus, resulting in about 6.8 million deaths. Early detection of the disease is crucial for providing care and reducing the rise in death rates in various countries, in addition to the spread of COVID-19. The two vital ways for COVID-19 detection are the Real-Time Reverse Transcription-Polymerase Chain Reaction (RT-PCR), which recognizes the genetic material of the infection, and the method which recognizes the protein from the virus is called Rapid Antigen Test

Received 4 June 2023; revised 29 August 2023; accepted 8 September 2023.
Available online 27 December 2023

* Corresponding author.
E-mail address: hagerhesham653@gmail.com (H.H. Eldawoudy).

<https://doi.org/10.58491/2735-4202.3116>

2735-4202/© 2024 Faculty of Engineering, Mansoura University. This is an open access article under the CC BY 4.0 license (<https://creativecommons.org/licenses/by/4.0/>).

(RAT). Blood samples were examined for particular proteins of the COVID-19 virus using the RAT technique. It is less accurate than PCR tests when there are no symptoms or when the amount of virus is low because antibodies might take 9–20 days to appear, so this technique of testing for COVID-19 is ineffective.

Another method for detecting COVID-19 is RT-PCR, which detects the genetic material called RNA (ribonucleic acid) from the virus in the sample and must be transformed into DNA (deoxyribonucleic acid) for amplification, which is achieved using RT-PCR, and this process takes 6–9 h to perform (Shyni and Chitra, 2022). They have several limitations, including a lack of testing kits during a crisis, a sensitivity of about 60–70%, making it a risky option, and the fact that it has resulted in false negatives in many case scenarios (Long et al., 2020).

The medical field requires available screening techniques to diagnose SARS-CoV-2 properly. Because the symptoms of COVID-19 are similar to those of other chest diseases, imaging methods are essential for prediction and diagnosis, monitoring disease severity, and evaluating the treatment response. There are several medical imaging procedures available, including computed tomography (CT), ultrasonography, and CXR images. Because the lung region is the most commonly affected by the virus, it is frequently used to determine the severity of the disease (Ai et al., 2020). Chest CT scans are a method of scanning the chest to detect COVID-19. They provide more precise information about the lung area that is infected as well as being a more sensitive and highly accurate scan. The rays emitted by CT scans are so much more dangerous to someone's health than those emitted by X-rays (Li and Xia, 2020). X-ray imaging modalities are just another useful technique used in the diagnosis of COVID-19 and other respiratory infections because of their quick processing duration, cheapness, security, reliability, and efficacy (Cozzi et al., 2020). An example of a CXR scan and a CT scan image is depicted in Fig. 1.

Deep learning (DL) is a subclass of machine learning (ML), and ML is a subclass of artificial intelligence (AI) that is built on artificial neural networks (ANNs). The ANNs contain many different layers, such as input, hidden, and output layers, so the network is called 'deep,' and the learning process is complex. There are three main types of learning processes, supervised, unsupervised, or semi-supervised (Gupta, 2018). Fully automated and real-time radiography image analyses based on DL methodologies are essential to assist physicians in accurately diagnosing COVID-19 infections. It helps physicians analyze COVID-19 symptoms that are not visible to the human eye on a CXR, as well as time and effort protection. Deep neural networks, especially convolutional neural networks (CNNs), are among the most important methodologies used in computer vision and medical imaging techniques (Yamashita et al., 2018). DL has been used for the diagnosis of various diseases such as eye tumors (Allam et al., 2022), skin cancer (Kadampur and Al Riyae, 2020), breast cancer (Amrane et al., 2018), diabetic retinopathy (Alyoubi et al., 2020), brain tumors (Amin et al., 2022), and lung and chest diseases (Abiyev and Ma'aitah, 2018) using image information such as CTs, CXRs, and magnetic resonance imaging techniques. In the present study, a DL model is proposed for automatic COVID-19 detection using an imaging technique named CXR images. We collect 11,100 CXR images from the Kaggle website and are split into three classes such as COVID-19, normal, and pneumonia classes. The dataset is balanced, meaning that the number of images in each class is equal to the number of images in the other classes. The proposed model is considered a stacked ensemble model based on LR for three pretrained models such as ResNet-152, DenseNet-201, and Vgg-19. Our research aims to use ensemble techniques to improve the model's performance to a higher level than other single models. For evaluations, we use different optimizers, such as Adam, Adagrad, ASGD, and SGD optimizers. Finally, we compare the results and the



Fig. 1. Examples of CXR and CT images.

proposed model with the SGD optimizer, which achieves the highest accuracy. The following is a summary of this paper's major contributions:

- (1) A large dataset of CXR images is collected from the Kaggle website, which is widely available and detects disease faster than traditional testing techniques such as RT-PCR.
- (2) Deep features are extracted from input CXR images using Transfer Learning (TL) models such as VGG-19, ResNet-152, and DenseNet-201 as base models that are ensembled for COVID-19 detection.
- (3) In this study, a stacked EM based on LR is proposed for COVID-19 detection from CXR images to improve performance and achieve optimal prediction.
- (4) Comparisons between the proposed model and the other existing models can be made using various performance metrics such as accuracy, precision, recall, the F1-score, and the AUC that are used for evaluation and making the model more robust.

The idea of our proposed model and how it was implemented and utilized in this study are discussed in detail in Section D. The remaining portion of the paper is divided into sections. Section II describes the briefly related works of other studies about different technologies that were utilized in COVID-19 detection. Section III contains details of the collected data, the preprocessing stages, the pretrained models, and the proposed model framework is fully detailed. Section IV provides us with results obtained from performance metrics used in evaluating the proposed model. Lastly, the conclusions are found in Section VI.

2. Related work

Since the global spread of the COVID-19 pandemic, DL models have been widely used for detecting COVID-19.

From chest imaging techniques such as CXRs and CTs < AQ: Pls check whether text missing here>. In this section, we presented several studies that used DL techniques to provide rapid detection of COVID-19 disease. They are also used in helping medical professionals work to keep diseases from spreading (Sethy and Behera, 2020). An ensemble model was developed by Kundu and colleagues (Kundu et al., 2021) for COVID-19 detection. This model was used with Sugeno to integrate the features of the four pretrained models: Wide ResNet-50-2, SqueezeNet v1.1, GoogLeNet, and VGG-11. They collected their

dataset, which reached 2481 images and was divided into two classes (1252 for COVID and 1229 for non-COVID). Their model was evaluated, and the performance accuracy reached 98.93%. Roy and Kumar (2022) suggested an ensemble model based on TL with dropout and four FC layers with 512, 256, 128, and 64 neurons, respectively, and combining their neurons. The suggested technique consisted of seven DL models that have been combined, such as Inception-v3, Xception, ResNet-50, DenseNet-201, VGG-16, VGG-19, and MobileNet-v2, used in COVID-19 detection. They collected 2000 images of chest X-rays (CXR) (1000 images of COVID-19 patients and 1000 images of normal patients). Their dataset was split into three sets, such as a training set (1200 images), a testing set (400 images) and a validation set (400 images). Their model was applied to predict COVID-19 from CXR images and achieved 99.99% accuracy.

A CoviXNet model was presented by Srivastava and colleagues (Srivastava et al., 2022) and consisted of a 15-layer CNN architecture that was used in screening the COVID-19 disease from the CXR imaging technique. Their dataset was gathered from different repositories, which contained 6207 images (1281 COVID-19 images, 3270 normal images, and 1656 viral pneumonia images). CoviXNet achieved a 10-fold accuracy in binary and multi-classification of values of 99.47% and 96.61%, respectively. They also used pretrained models to detect COVID-19 from CXR images, such as EfficientNet-B0 and B1 and Inception-v3, achieving an accuracy of 99.78% on binary classification. The EMCNet model was suggested by Saha and colleagues (Saha et al., 2021) for detecting COVID-19 disease from CXR images. The high-level features were extracted from CXR images using EMCNet and CNN, and then classified using an ensemble model of four different ML classifiers. Random forest, support vector machine (SVM), decision tree, and AdaBoost were the classifiers used in their research, and the outputs of these classifiers were combined with the input of the ensemble classifier. The total number of images in their dataset reached 4600 images (2300 COVID-19 images and 2300 normal images) and was divided into 70% training, 20% validation, and 10% testing. Their model was evaluated, and its accuracy reached 98.91%. A deep ensemble model was suggested by Das and colleagues (Das et al., 2021) and was employed to diagnose COVID-19 patients using CXR images. The ensemble model was utilized to ensemble the features of the pretrained models such as Inception-v3, DenseNet-201, and ResNet-50v2. Their dataset was divided into three sets: 771 for training, 118 for testing, and 117 for validation, with

a total of 538 images of COVID-19-positive images and 468 images of normal images. Their model was evaluated and obtained a 91.62% accuracy.

An ensemble model was developed by Mahanty and colleagues (Mahanty et al., 2022) that was used for the classification of CT images into COVID-19, pneumonia, and normal classes. The Sugeno fuzzy integral method was used to ensemble the features of the three pretrained models, such as MobileNetV2, SqueezeNet, and DenseNet-201. They used CT image datasets for evaluation, which were split into two sets: a training set and a testing set. Their dataset contained 1687 normal images, 1468 images of pneumonia and 999 COVID-19 patient images. The MobileNetV2 with the trainable ensemble and the Sugeno fuzzy integral achieved the highest accuracy of 98.80% and 99.15%, respectively. An ensemble classifier called EDL-COVID was suggested by Zhou and colleagues (Zhou et al., 2021), which was designed to detect COVID-19 from CT images.

The ensemble model was used to fuse the features of three pretrained models, such as AlexNet, GoogleNet, and ResNet, and the Softmax layer was used for the classification process. The 7500-CT image was used and divided into two sets, with 80% of them being the training set, and 20% of them being the testing set. They compared the performance metrics of the EDL-COVID model to those of the other three pre-trained models, and the ensemble model achieved the highest accuracy of 99.054%. An ensemble model was suggested by Solaiman and colleagues (Solaiman et al., 2022) and used in combining the features of five pretrained models, including NasNetLarge, VGG-19, Inception-ResNet-v2, DenseNet-201, and Xception. They evaluated their model using the CXR dataset, which was divided into two sets: training (80% of the dataset) and testing (20% of the dataset), and was also divided into three classes. The highest accuracy was achieved from the ensemble model among the pretrained models, reaching an accuracy of 96.25%. An ensemble model was designed by Kini and colleagues (Kini et al., 2022) that used fine-tuning models, including ResNet-152-V2, Inception-ResNet-v2, and DenseNet-201, for COVID-19 detection from the CT imaging technique. They evaluated their model on four classes containing 2839 images of COVID-19, 3482 normal images, 2632 tuberculosis images, and 3193 pneumonia chest CT scan images, and divided their dataset into a 65% training set and a 35% testing set. They calculated the performance metrics of the ensemble models, achieving an accuracy of 98.98%.

The authors in AbdElhamid and colleagues (AbdElhamid et al., 2022) suggested a model with a

GAP layer to reduce the overfitting and an activation layer to reduce losses. They used several optimizers to evaluate the model, such as AdaGrad, AdaDelta, SGD, RMSprop, Adam, and Adamax. Their testing dataset was compiled from various Kaggle repositories and included 1751 for normal, 1371 for COVID-19, and 4273 for pneumonia. Model validation was performed using the testing data and the highest performance metric was achieved with an accuracy of 99.3%.

LW-CORONet was designed by Nayak et al. (2023) and used in the accurate detection of COVID-19 from CXR images. Their model was effective because it required less memory space, had fewer parameters, and allowed for easy feature extraction from CXR images. It used only five learnable layers such as convolution, batch normalization, RELU, pooling, and finally, there is the fully connected layer. They collected two COVID-19 CXR datasets from various data repositories were utilized for model assessment. The first dataset contained 2250 images, such as 750 for normal, 750 for pneumonia, and 750 for COVID-19. The second dataset contained 15,999 images, such as 8066 for normal, 5575 for pneumonia, and 2358 for COVID-19. Their model was evaluated based on their datasets, and their accuracy reached 98.67% and 99.00% on the first dataset, and 95.67% and 96.25% on the second dataset for multi and binary-class classification, respectively. An ensemble model was designed by Kumar and colleagues (Kumar et al., 2023) for accurate COVID-19 detection by combining three pretrained models such as GoogLeNet, EfficientNet, and XceptionNet. Their model was evaluated on two datasets collected from different repositories and was able to classify them into four categories: pneumonia, COVID-19 (+), tuberculosis, and normal. Two experiments were performed and showed us that their model could classify binary and multiclass classifications. Their model was assessed, and it achieved 99.21% accuracy for multiclass classification and 98.95% accuracy for binary classification, respectively. Multiclassification DL models were designed by Ibrahim and colleagues (Ibrahim et al., 2021) and were used in COVID-19 detection using CT and CXR images. Several DL models were used in their study, including ResNet152V2+Bi-GRU, VGG19 + CNN, ResNet152V2+GRU, and ResNet152V2. These models were capable of categorizing diseases into four categories, such as 'normal,' 'COVID-19,' 'pneumonia,' and 'lung cancer.' Several data sources were used for gathering the datasets and divided into two sets: 70% of the dataset was split as a training dataset, and 30% of the dataset was split as

a testing dataset. The highest accuracy was achieved by VGG19 + CNN, which was 98.05%.

After the COVID-19 pandemic, various studies developed DL models for COVID-19 detection utilizing imaging techniques such as CXRs and CTs. The use of DL provides us with an accurate technique for detecting COVID-19, and it differs from traditional methods in that it has an end-to-end architecture that does not need any feature extraction methods. These studies, discussed in this section, used various techniques for COVID-19 detection, including single models, TL, and ensemble learning models, each of which has advantages and disadvantages. One of these limitations was that studies that used ResNet, MobileNet, and VGG-19 pretrained models had a large number of trainable parameters, which caused a large computational cost. Furthermore, the huge several research papers only have a small amount of data, so additional data is needed to improve the accuracy and reliability of models. In our study, we suggested an ensemble model of three pretrained models, such as VGG-19, DenseNet-201, and ResNet-152, to prevent overfitting problems. To enhance the model's performance with the fewest losses, we collected a larger dataset from various repositories on the 'Kaggle' website and used it for model evaluation.

3. Materials and methods

Our proposed ensemble model is based on detecting COVID-19 in infected people from CXR

images. Its final prediction is greater than the predictions of every single model because it combines the prediction values of the three pretrained DL models, such as VGG-19, DenseNet-201, and ResNet-152. The suggested model's structure is presented as a block diagram, as shown in Fig. 2, and discussed in the subsections that are below.

3.1. Data preparation and preprocessing

In our study, a dataset of CXR images is gathered from four publicly available data repositories that are available on the 'Kaggle' website:

- (1) Chest Radiograph Images (pneumonia) (Mooney, 2018).
- (2) COVID-19 Radiography Database (Rahman, 2020).
- (3) COVID Chest Radiograph Dataset (Cohen, 2020).
- (4) COVID-19 Image Dataset (Raikote, 2020).

A total of 11100 images are collected and prepared from these data repositories (3700 for COVID-19, 3700 for normal, and 3700 for pneumonia) that are used for multiclassification in detecting COVID-19 from CXR images. Fig. 3 shows us samples of COVID-19, normal, and pneumonia CXR images.

The first step in data preparation is data preprocessing (Al-Shourbaji et al., 2023), which is used to improve the data by removing noise and distortion and making the network more effective and faster. The gathered dataset is in a variety of sizes,

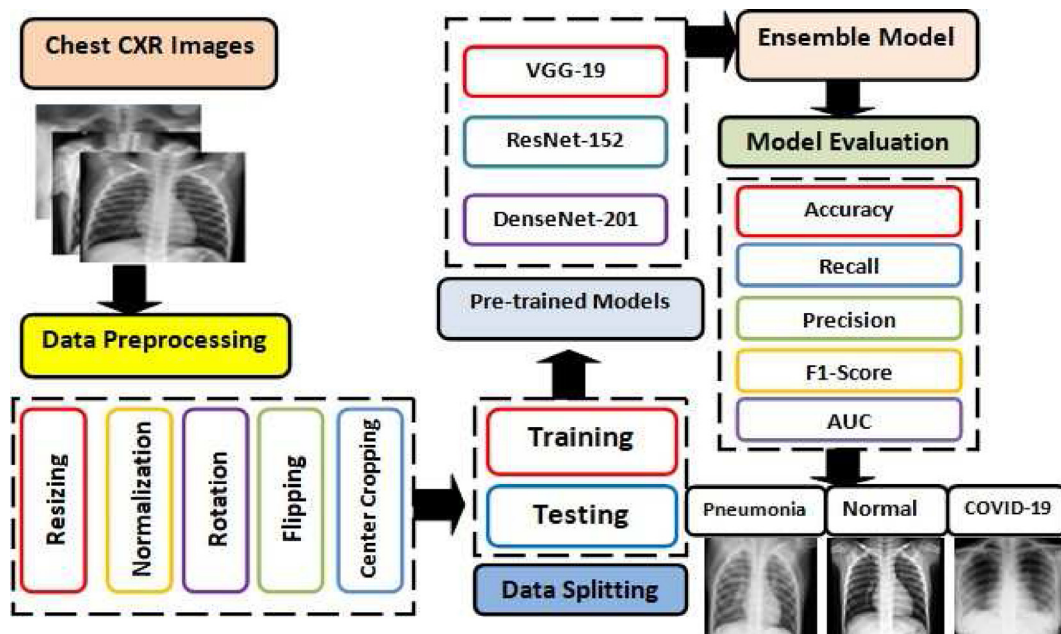


Fig. 2. A block diagram of the structure of the proposed ensemble model using CXR images.

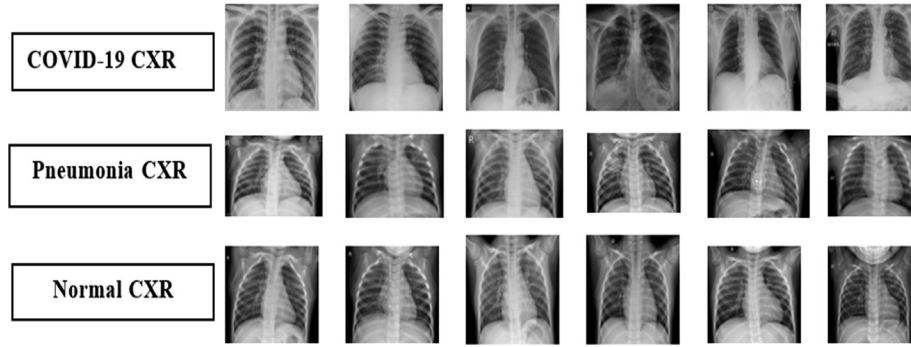


Fig. 3. Examples of COVID-19, normal, and pneumonia CXR images.

so we resized it to a standard size of 128×128 pixels. Each image has pixel values ranging from 0 to 255, and the process becomes complex when the image passes through the CNN. We use normalization to minimize complexity by dividing all values by 255, resulting in a range of $[0, 1]$. The normalization process is discussed in Equation (1), where N_d is the normalized data; D is the original data; D_{max} is the max value of the input data; and D_{min} is the min value of the input data. Owing to data leakage, we utilize data augmentation to enlarge the training dataset and reinforce the model. Also, we apply rotation up to a maximum of 10° , with a probability of 0.4 the images will be flipped horizontally. Furthermore, center cropping performs a crop at the center of the CXR images. Fig. 4 shows us an example of CXR images after and before data augmentation and normalization:

$$N_d = \frac{D - D_{min}}{D_{max} - D_{min}} \quad (1)$$

Then, we split our dataset into two sets. The first set is about 70% of the dataset which is called a

training set, and the second set is about 30% of the dataset, which is called a testing set, and is discussed in detail as shown in Table 1. The pie chart 5 shows us the percentage distribution of COVID-19, normal, and pneumonia classes. (The pie chart in Fig. 5 shows us the percentage distribution.)

3.2. Deep transfer learning

The proposed model uses three pretrained DL models, which are trained on a large-scale ImageNet dataset and it includes 14 million images and can classify them into 1000 classes. The deep TL models used in this study are as follows:

- (1) VGG-19: It is a convolutional neural network that was developed by Simonyan, Zisserman (Simonyan and Zisserman, 2015) and more than a million images from the ImageNet database were used to train (Deng et al., 2009). The pre-trained model has 19 layers including three fully connected layers and 16 convolutional layers for feature extraction. It can classify the images into 1000 different item classes. The network's input

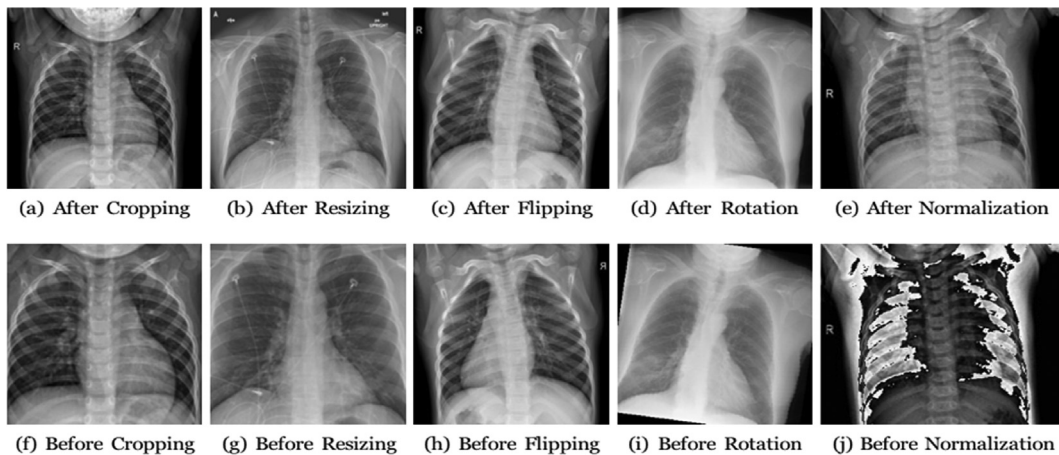


Fig. 4. CXR images after and before data augmentation and normalization.

Table 1. Splitting the dataset into a training set and a testing set.

Splitting data	COVID-19	Pneumonia	Normal
Training Set	2590	2590	2590
Testing Set	1110	1110	1110
Total	3700	3700	3700

has a 128*128-sized RGB image and is passed through the convolution layers for the processing process. Each convolutional layer has several 3×3 filters that are used to extract the image's deep features. A max-pooling layer is placed after the convolution layers and is used to minimize the feature map's size. The last layer that is used to predict the probability for all classes is the LogSoftmax layer.

- (2) DenseNet-201: It is a deep convolutional neural network that was proposed by Huang and colleagues (Huang et al., 2018). It was trained on more than a million images from the ImageNet database (Deng et al., 2009) and can categorize images into 1000 classes. The input image to the network is 128 by 128 in size, and the pretrained model contains 201 layers. Each layer of the network contains batch normalization, RELU activation function, and convolution with a 3*3 filter. Batch normalization is a technique that helps us reduce overfitting during training while also making the training process faster and more reliable. Any negative value is turned into zero by the nonlinear ReLU (rectified linear unit) function. There is a pooling layer at the end of the last dense layer that is used to reduce the future map's features. Following the pooling layer, a LogSoftmax classifier helps us in determining each class's probability.

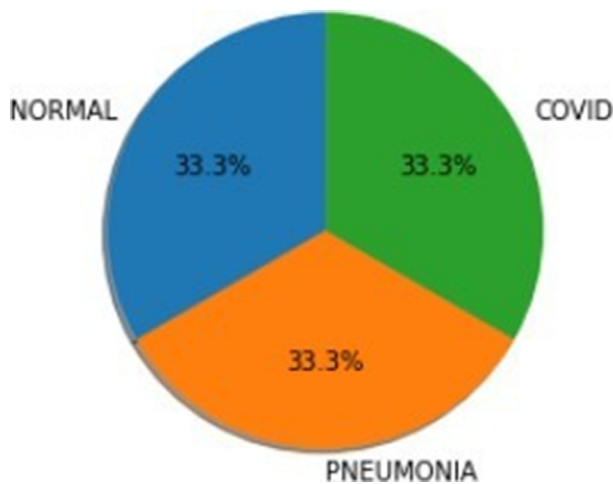


Fig. 5. Percentage distribution of COVID-19, normal, and pneumonia classes.

- (3) ResNet-152: It is a deep CNN with 152 layers that are based on the deep residual network (residual network, ResNet) (He et al., 2016). The residual network is described as adding many residual blocks, which aims to broaden the neural network's depth. This strategy can increase model performance while also improving training speed. ResNet152 is pretrained on the ImageNet dataset, and an input image into the network is 128 by 128 pixels in size. It consists of 50 blocks and each block has three layers and then a pooling layer that is used to decrease the features of a future map. The final layer is the LogSoftmax layer, which predicts each class's probability.

3.3. Deep learning optimizers

Optimizers are algorithms used during the training process that adapt the learnable parameters, such as learning rate and weights (Musstafa, 2021). They are used to reduce losses or error functions while increasing accuracy. We used different optimizers to select the best values for learning rate and weights. The DL optimizers used in this study are as follows:

- (1) Adam Optimizer: It is a gradient-descent optimization technique that is also known as Adaptive Moment Estimation (Khandelwal, 2019). It is a technique that takes the first and second moments calculated from the gradients and then computes the adaptive learning rates for each parameter. Adam is a hybrid technique that combines the advantages of a momentum-based GD optimizer (Bhat, 2020) and RMSProp optimizer (root-mean-square prop) (Sanghvirajit, 2021). Adam, like RMS-Prop, maintains the decaying average of the past gradients as momentum, as well as the decaying average of the past squared gradients, and provides the adaptive learning rate of RMS-Prop, making Adam a robust technique.
- (2) AdaGrad Optimizer: It is called the Adaptive Gradient Algorithm and is an optimization algorithm to accelerate the training of deep neural networks and improve their performance (Oppermann, 2023). It is a method of stochastic optimization that adjusts the learning rate of each parameter during the training process of the neural network adaptively. In an optimizer such as SGD with momentum, the learning rate remains constant, but in the AdaGrad optimizer, which has no momentum, it is simpler than SGD

with momentum. It can better handle sparse data because its input features have a low frequency, and Adagrad is capable of adjusting the learning rate of each parameter to make it higher.

- (3) SGD Optimizer with Momentum: It is also known as the Stochastic Gradient Descent with Momentum Deep Learning Optimizer (Mayanglambam, 2020). SGD has a high oscillation, which causes it to fall to a minimum. Also, because the learning rate did not increase, it took time to converge, resulting in poor performance. However, the SGD with momentum solves this problem using exponentially weighted averages to compute the gradient that was used to update the parameter, which overcomes the noisy gradient, reduces oscillations, and accelerates the SGD to converge quickly.
- (4) ASGD Optimizer: It stands for Averaged Stochastic Gradient Descent Optimizer (Srivastava, 2022), which accelerates stochastic approximation by averaging the weights that are produced in each iteration.

3.4. Proposed stacked ensemble model

Ensemble learning is a hybrid learning system that combines the predictions of many pretrained models to produce better results than an individual pretrained model. Ensemble learning is classified into three types: bagging, boosting, and stacking (Rodge, 2021). Stacking is an improved strategy of the ensemble techniques based on training the base models (bm) in parallel, and their predictions are combined as features and used as an input to the meta-learner model. Stacking can be done by splitting the dataset into training and testing sets.

The training set is divided into K folds, after which the base models are trained on K-1 folds as a training set and predictions are made on the Kth fold as a testing set. Finally, the predictions from the base learners are used as features as input to the meta-learner model to make the optimal final prediction.

Our model is proposed as a stacking ensemble architecture that is shown in Fig. 6 and consists of two-level models. The first-level model is a combination of base learner models such as ResNet-152, DenseNet-201, and Vgg-19, while the second-level model is the meta-learner model, which considers an LR followed by an activation function such as a ReLU function. Our input training dataset X is split into five folds. In every iteration, each base model is trained on four folds, and the fifth fold is used for testing the model. Then, every base model which is known as bm is described as a function F_{bm}^i , which evaluates the predictions of each base model which are known as P_{bm}^i as shown in Equation (2) on input data at every iteration i , where $i = 1, 2, 3, 4,$ and 5 .

$$P_{bm}^i = F_{bm}^i(H_i) \quad (2)$$

where H_i describes the holdout dataset at every iteration i . Iteratively, the process is repeated until each H_i is predicted. The first-level models predict $P_1, P_2,$ and P_3 of the VGG-19, DenseNet-201, and ResNet-152, respectively. The LR model is chosen as a meta-learner model, which explains the linear relationship between the features and the predictions of base models. It is trained on the first-level predictions of base models to produce the optimal prediction. Then the meta-learner will 'stack' the predictions $P_1, P_2,$ and P_3 by a linear combination with weights W_i , which is discussed in equations (3) and (4).

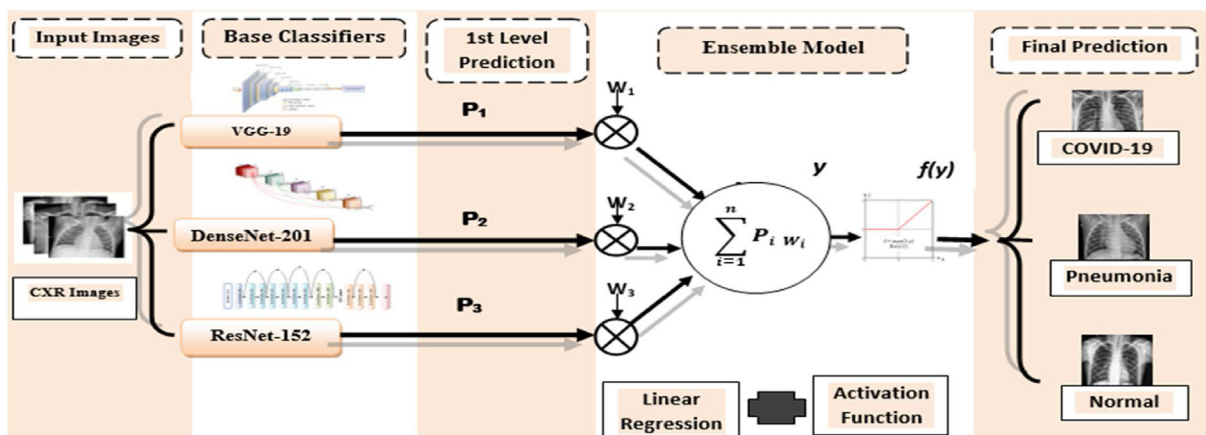


Fig. 6. A framework of the proposed Stacked Ensemble model.

Table 2. Precision, Recall, F1-score, and AUC performance metrics of ResNet-152, DenseNet-201, VGG-19, and the proposed ensemble model (EM) with different optimizers: (a) Adam, (b) AdaGrad, (c) ASGD, and (d) SGD.

Model	Class	Opt	Prec	Recall	F1	AUC	Opt	Prec	Recall	F1	AUC
ResNet152	COVID-19	Adam	1.00	0.97	0.99	0.99	AdaGrad	0.92	1.00	0.96	0.98
	Pneumonia		1.00	0.77	0.87	0.89		1.00	0.94	0.97	0.97
	Normal		0.80	1.00	0.89	0.94		0.94	0.91	0.93	0.94
	Macro Avg		0.93	0.91	0.91	0.94		0.95	0.95	0.95	0.96
	Weighted Avg		0.93	0.91	0.91	NA		0.95	0.95	0.95	NA
DenseNet201	COVID-19	Adam	0.85	1.00	0.92	0.96	AdaGrad	0.97	1.00	0.99	0.99
	Pneumonia		1.00	0.60	0.75	0.80		0.94	0.97	0.96	0.97
	Normal		0.74	0.91	0.82	0.88		1.00	0.94	0.97	0.97
	Macro Avg		0.87	0.84	0.83	0.88		0.97	0.97	0.97	0.98
	Weighted Avg		0.87	0.84	0.83	NA		0.97	0.97	0.97	NA
VGG19	COVID-19	Adam	0.92	0.94	0.93	0.95	AdaGrad	0.82	0.94	0.88	0.92
	Pneumonia		0.97	0.86	0.91	0.92		0.91	0.91	0.91	0.94
	Normal		0.82	0.89	0.85	0.89		0.83	0.71	0.77	0.82
	Macro Avg		0.90	0.90	0.90	0.92		0.86	0.86	0.85	0.89
	Weighted Avg		0.90	0.90	0.90	NA		0.86	0.86	0.85	NA
EM	COVID-19	Adam	1.00	0.97	0.99	0.99	AdaGrad	1.00	1.00	1.00	1.00
	Pneumonia		0.97	0.91	0.94	0.95		1.00	0.97	0.99	0.99
	Normal		0.89	0.97	0.93	0.96		0.97	1.00	0.99	0.99
	Macro Avg		0.95	0.95	0.95	0.96		0.99	0.99	0.99	0.99
	Weighted Avg		0.95	0.95	0.95	NA		0.99	0.99	0.99	NA
ResNet152	COVID-19	ASGD	1.00	1.00	1.00	1.00	SGD	1.00	0.97	0.99	0.99
	Pneumonia		1.00	0.89	0.94	0.94		0.95	1.00	0.97	0.99
	Normal		0.90	1.00	0.95	0.97		1.00	0.97	0.99	0.99
	Macro Avg		0.97	0.96	0.96	0.97		0.98	0.98	0.98	0.99
	Weighted Avg		0.97	0.96	0.96	NA		0.98	0.98	0.98	NA
DenseNet-201	COVID-19	ASGD	1.00	1.00	1.00	1.00	SGD	1.00	1.00	1.00	1.00
	Pneumonia		0.97	0.97	0.97	0.98		0.97	1.00	0.99	0.99
	Normal		0.97	0.97	0.97	0.98		1.00	0.97	0.99	0.99
	Macro Avg		0.98	0.98	0.98	0.99		0.99	0.99	0.99	0.99
	Weighted Avg		0.98	0.98	0.98	NA		0.99	0.99	0.99	NA
VGG-19	COVID-19	ASGD	1.00	0.94	0.97	0.97	SGD	0.97	1.00	0.99	0.99
	Pneumonia		1.00	0.69	0.81	0.84		1.00	0.97	0.99	0.99
	Normal		0.73	1.00	0.84	0.91		0.97	0.97	0.97	0.98
	Macro Avg		0.91	0.88	0.88	0.91		0.98	0.98	0.98	0.99
	Weighted Avg		0.91	0.88	0.88	NA		0.98	0.98	0.98	NA
EM	COVID-19	ASGD	1.00	1.00	1.00	1.00	SGD	1.00	1.00	1.00	1.00
	Pneumonia		1.00	0.97	0.99	0.99		1.00	1.00	1.00	1.00
	Normal		0.97	1.00	0.99	0.99		1.00	1.00	1.00	1.00
	Macro Avg		0.99	0.99	0.99	0.99		1.00	1.00	1.00	1.00
	WeightedAvg		0.99	0.99	0.99	NA		1.00	1.00	1.00	NA

Table 3. Average accuracy of ResNet-152, DenseNet-201, VGG-19, and the proposed ensemble model (EM) with different optimizers: (a) Adam, (b) AdaGrad, (c) ASGD, and (d) SGD.

Model	Optimizer	Accuracy	Optimizer	Accuracy
ResNet152		91.43%		95.24%
DenseNet201	Adam	83.81%	AdaGrad	97.14%
VGG-19		89.52%		85.71%
EM		95.24%		99.05%
ResNet152		96.16%		98.10%
DenseNet201	ASGD	98.10%	SGD	99.05%
VGG-19		87.62%		98.10%
EM		99.05%		100%

The purpose of using LR with a stacked Ensemble Model is that LR explains only the linear relation between features and predictions and does not learn the nonlinear relationship. For this reason, we use the activation function like the ReLU function to explain the nonlinear relationship between features and predictions. The ReLU function is the rectified linear unit that is used as an activation function in DL models. If the input value is negative, the output value is zero, and if the input value is positive, it returns to the input value, as discussed in equation (5).

Finally, apply the linear transformation after applying the RELU activation function that is used for predicting the final prediction:

$$F_{stacking} = \sum_{i=1}^n W_i * P_{bm} \quad (3)$$

where n represents the number of models trained.

$$y = F_{stacking} = W_1 * P_1 + W_2 * P_2 + W_3 * P_3 \quad (4)$$

$$Z = f(y) = y \text{ if } y \geq 0 \text{ \& } 0 \text{ if } y < 0 \quad (5)$$

4. Performance evaluation

The confusion matrix is a method for evaluating the model's performance that is used in binary and multiclass classification tasks based on test datasets. It is an $M \times M$ matrix, where M is the number of target classes and represents the actual and predicted values of the given classes in the testing set. Each column of the confusion matrix shows us the model's predictions, and each row represents the actual classes. We evaluate our model using a 'normalized confusion matrix,' which refers to converting all of the outcome values for each class in the model's confusion matrix into a percentage value. Each row is divided by the total sum of the entire row to be normalized. There are other metrics used in comparing the proposed model to other

models to evaluate how well classification techniques work (Vidiyala, 2020). These metrics are accuracy, recall, precision, specificity, and F1 score, which are described in Equations (6)–(10), respectively.

Accuracy (A) is defined as the ratio of the sum of correctly labeled predictions to the total number of classified predictions:

$$A = \frac{t_N + t_P}{t_N + t_P + f_N + f_P} \quad (6)$$

Recall (R), sensitivity, or true positive rate (TP_R) is defined as the ratio of true positives to the total of true positives and false negatives:

$$R = \frac{t_P}{t_P + f_N} \quad (7)$$

Precision (P) is defined as the ratio of true positives to the total of true positives and false positives, and the precision should be high:

$$P = \frac{t_P}{t_P + f_P} \quad (8)$$

Specificity (S) is defined as the ratio of true negatives to the total of true negatives and false positives. The model's performance improves with increasing specificity:

$$S = \frac{t_N}{t_N + f_P} \quad (9)$$

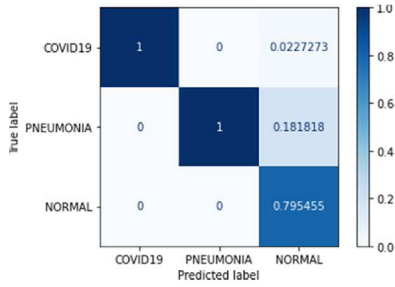
The F-measurement or F1 score (F1) is defined as the weighted average of precision and recall and is used to compare two models with high recall but low precision or low recall but high precision:

$$F1 = 2 * \left(\frac{R * P}{R + P} \right) \quad (10)$$

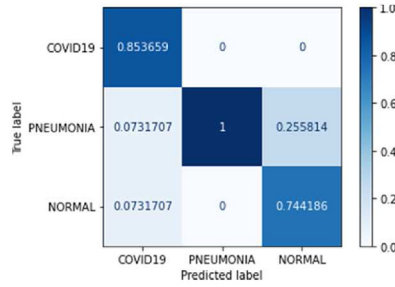
Another performance metric used in classification problems is called the AUC-ROC curve. The ROC curve (receiver-operating characteristic curve) is a graph that shows the performance of a model at all classification threshold levels by plotting the true positive rate (TP_R) across the x-axis and the false positive rate (FP_R) across the y-axis. The AUC metric measures the area under the ROC curve; the model performs better when the AUC is greater. Terms (TP_R) and (FP_R) used in the AUC-ROC curve are discussed in equations 7 and 11:

$$FP_R = \frac{f_P}{f_P + t_N} \quad (11)$$

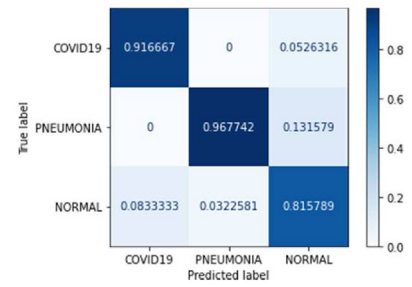
where t_P , t_N , f_P and f_N are as described below:



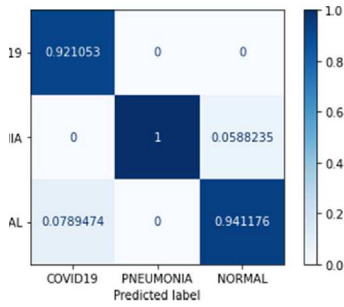
(a) ResNet152+Adam



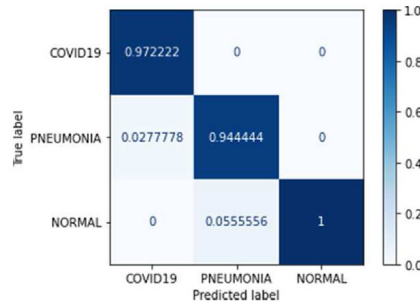
(b) DenseNet201+Adam



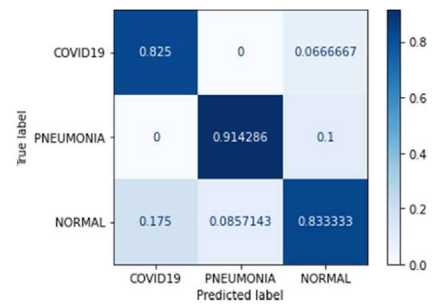
(c) VGG-19+Adam



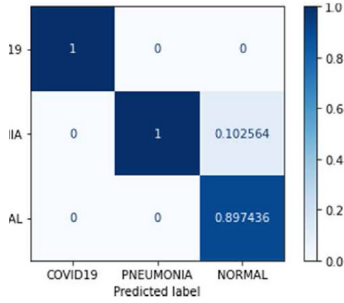
(d) ResNet152+AdaGrad



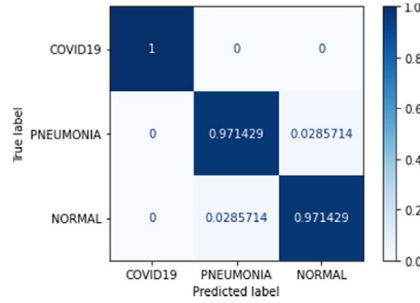
(e) DenseNet201+AdaGrad



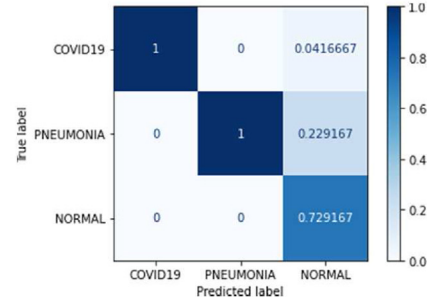
(f) VGG-19+AdaGrad



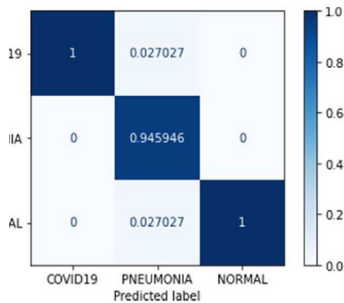
(g) ResNet152+ASGD



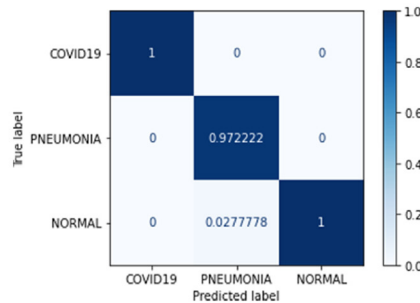
(h) DenseNet201+ASGD



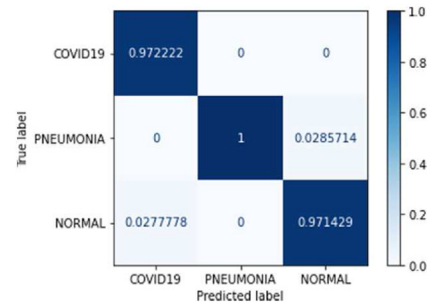
(i) VGG-19+ASGD



(j) ResNet152+SGD



(k) DenseNet201+SGD



(l) VGG-19+SGD

Fig. 7. Normalized confusion matrices of the ResNet-152, DenseNet-201, and VGG-19 pretrained models with different optimizers: Adam, (b) AdaGrad, (c) ASGD, and (d) SGD.

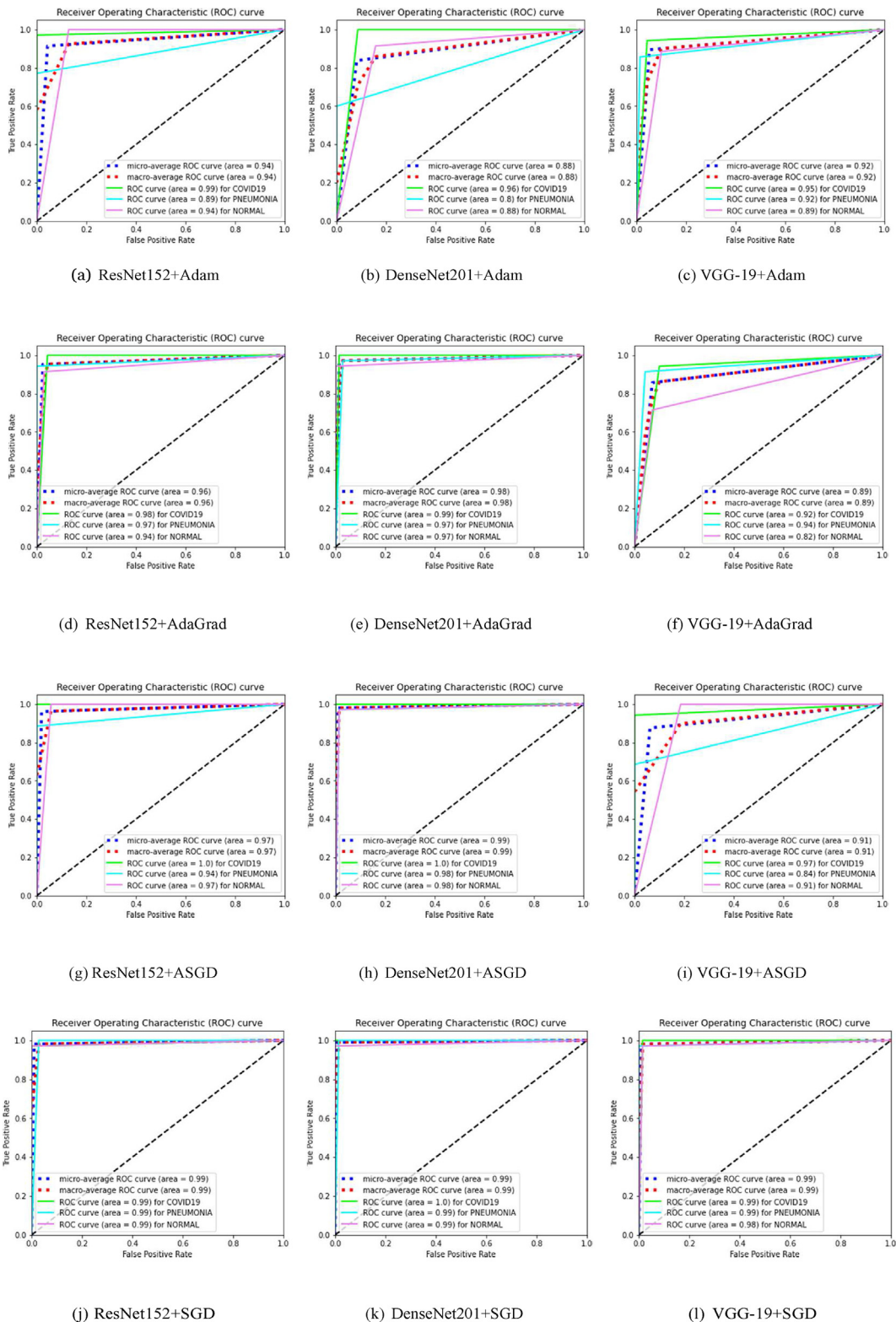


Fig. 8. ROC curves of the ResNet-152, DenseNet-201, and VGG-19 pretrained models with different optimizers: (a) Adam, (b) AdaGrad, (c) ASGD, and (d) SGD.

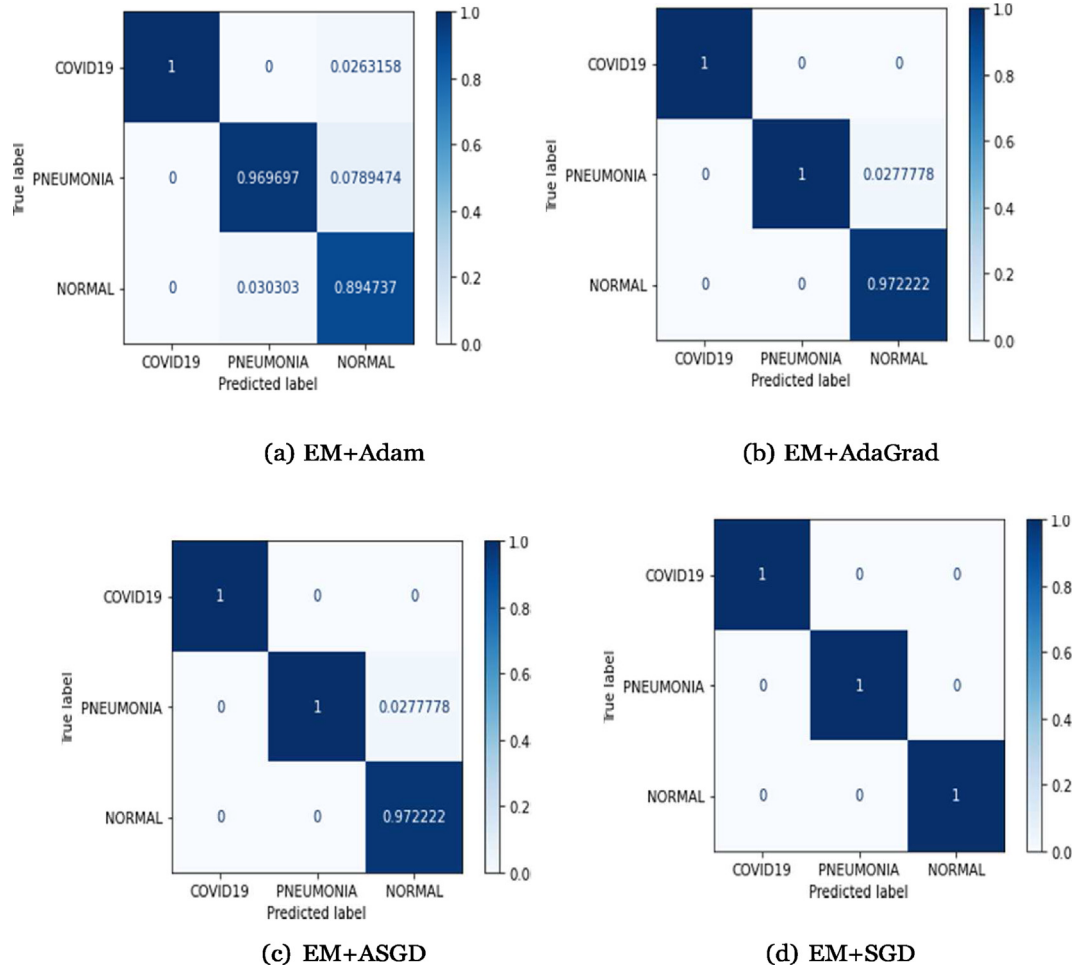


Fig. 9. Normalized confusion matrices of the proposed ensemble model (EM) with different optimizers: (a) Adam, (b) AdaGrad, (c) ASGD, and (d) SGD.

- (1) True positive (t_P): It indicates that a patient has COVID-19, and the model predicts the positive class correctly.
- (2) False positive (f_P): It indicates that a patient has COVID-19 and the model predicts the positive class wrongly; it is also called a 'type 1 error.'
- (3) True negative (t_N): It indicates that a patient does not have COVID-19, and the model correctly predicts the negative class.
- (4) False negative (f_N): It indicates that a patient does not have COVID-19 and the model predicts the negative class wrongly; it is also called a 'type 2 error.'

5. Experimental results

In this research, we used a stacked ensemble model as a meta-learner model, whose main idea is that a meta-stacked model performs better than other individual models. It is based on fusing the

predictions of the three pretrained models and learning them in parallel, such as ResNet-152, DenseNet-201, and Vgg-19. It is based on LR, which studies the linearity relation between the features and the predictions of the three base models. We used the 'PyTorch' open-source machine learning library for developing our model based on the Python programming language and the Torch library. The proposed model was trained with a learning rate of 0.01 and a batch size of 32, and training the model with six epochs. We gathered data from different websites on Kaggle, and these were split into two sets such as training and testing sets. The first set was the training set, which comprised approximately 70% of the dataset, and the second set was the testing set, which comprised 30% of the dataset. The image resizing technique into $128 \times 128 \times 3$ and data preprocessing was applied before inputting the neural network. In this work, our model was evaluated using various DL

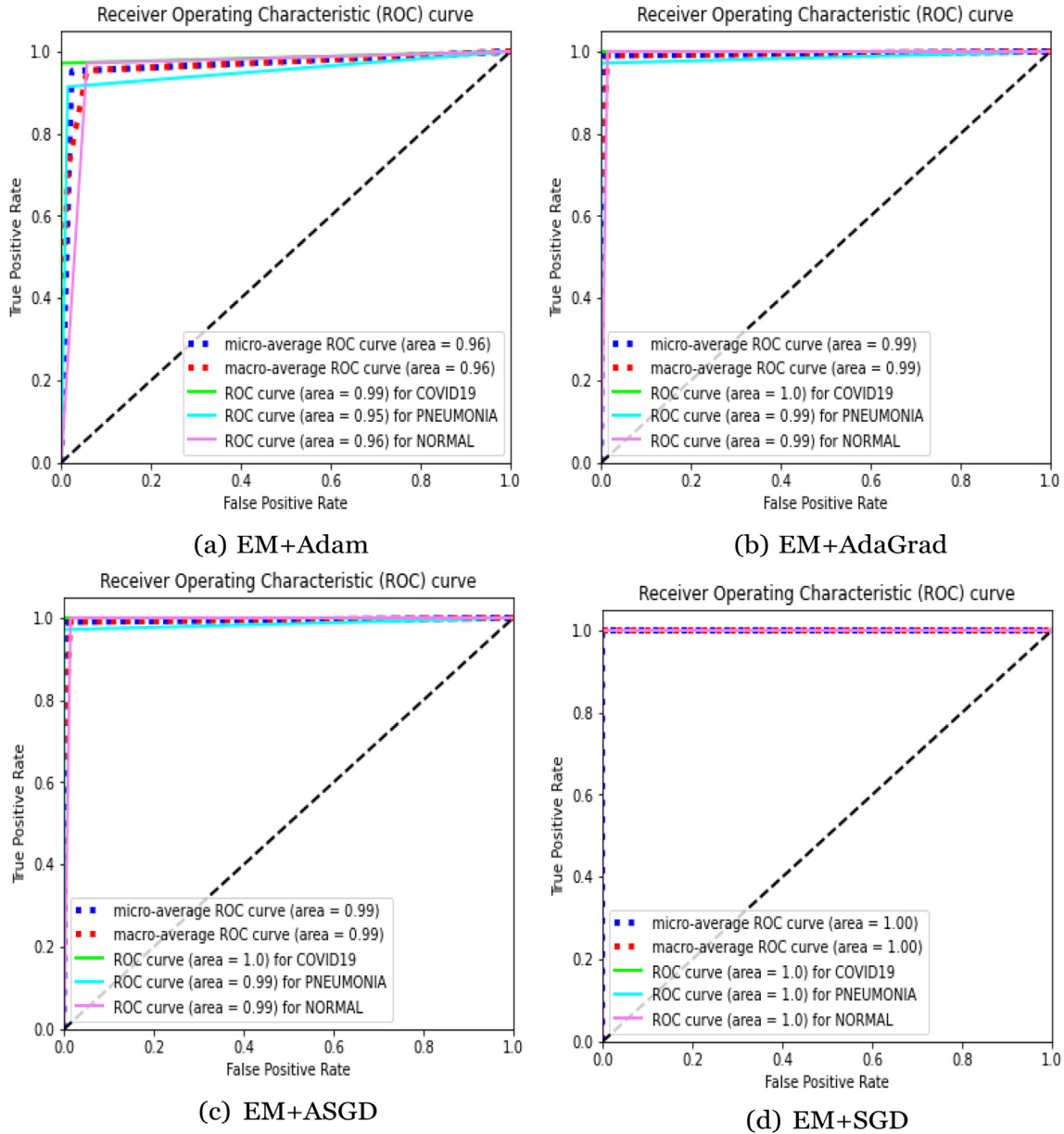


Fig. 10. ROC curves of the proposed ensemble model (EM) with different optimizers: (a) Adam, (b) AdaGrad, (c) ASGD, and (d) SGD.

optimizers like Adam, AdaGrad, ASGD, and SGD and compared their performance. Using the SGD optimizer with the proposed model resulted in improved performance accuracy and reduced losses. In our experiment, we evaluated the performance metrics of pretrained models and our proposed model using different optimizers and measuring the accuracy metric, as discussed in in Tables 2 and 3. The normalized confusion matrices and the ROC curves of the pretrained models with different optimizers are represented in Figs. 7 and 8. Furthermore, the normalized confusion matrices and the ROC curves of the proposed models with

different optimizers are demonstrated by Figs. 9 and 10. Finally, our approach's results for COVID-19 detection are promising when compared with previous DL studies as illustrated in Table 4. Roy and Kumar's study (Roy and Kumar, 2022) is the most comparable to our work because the difference in accuracy lies within the margin of statistical error, but it has some limitations. Our proposed model is an improvement on their suggested model, as we collected and used a larger dataset (11,100 images from 4 websites on Kaggle), unlike their study, whose dataset was quite small (2000 images from only one website on Kaggle). In addition to that, our

Table 4. Comparison of the proposed model with other DL methods using imaging techniques such as CXRs and CTs.

Ref	Year	Data Type	Classes	Data Splitting	Method	Results
Kundu et al. (2021)	2021	CT	2	70% train - 30% test	EM	Acc, Prec, Recall, Spec, F1 = 98.93%
Roy and Kumar (2022)	2022	CXR	2	60% train -20% test -20% val	EM	Acc 99.99%, Recall = 100%, AUC = 0.9999
Srivastava et al. (2022)	2022	CXR	2	70% train -20% test -10% val	CovixNetInceptionV3	Acc 99.47%, Acc = 99.78%, Recall = 100%
Saha et al. (2021)	2021	CXR	2	70% train -20% test -10% val	EMCNet	Acc 98.91%, Prec = 100%, Recall = 97.82%
Das et al. (2021)	2021	CXR	2	80% train -10% test -10% val	EM	Acc 91.62%, Recall = 95.09%, Spec = 88.33%
Mahanty et al. (2022)	2022	CT	3	70% train - 30% test	Fuzzy EM	Acc 99.15% =
Zhou et al. (2021)	2021	CT	3	80% train - 20% test	EDL-COVID	Acc, Recall 99.05%, Spec = 99.6% =
Solaiman et al. (2022)	2022	CXR	3	80% train - 20% test	EM	Acc 96.25% =
Kini et al. (2022)	2022	CT	4	65% train - 35% test	EM	Acc 98.98%, Prec = 98.56%, Recall = 98.58%
Abdelhamid et al. (2022)	2022	CXR	3	-80% train -10% test -10% val	Xception + GAP	Acc, F1 99.3%, Prec, Recall = 99%
Nayak et al. (2023)	2022	CXR	3	80% train - 20% val	LW-CORONet	Acc, F1 99%, Prec = 98.82%
Kumar et al. (2023)	2023	CXR	4	68% train -15% test -17% val	EM	Acc 99.21%
Ibrahim et al. (2021)	2021	CXR,CT	4	70% train - 30% val	VGG19 + CNN	Acc, Recall 98.05%, Prec = 98.34%
Proposed model	2023	CXR	3	70% train - 30% val	EM	Acc, Prec, Recall, F1, AUC = 100%

approach is more simple in structure as it is composed of three pretrained models, whereas their model is composed of seven pretrained models, which means heavy computation requirements. Also, our model can classify the images into three classes: pneumonia, COVID-19, and normal, while their approach can only classify the images into a binary classification as COVID or normal. Finally, their model was tested on only 400 images, while ours was tested on 3330 images, which means our result is more accurate.

6. Conclusions and future directions

For accurate COVID-19 detection using CXR scans, this paper provides a multiclassification diagnostic system based on DL systems. Early detection of COVID-19 is vital for preventing the virus from spreading between people and around the world and determining the appropriate therapy for patients. This proposed model combines deep TL models based on the stacked ensemble technique using LR to achieve optimal accuracy compared with other single-base models. The suggested model ensembles the features of three pretrained models using deep TL techniques and a stacked ensemble model. The proposed model is evaluated using many optimizers, and the SGD

optimizer achieved an accuracy of about 100%. We intend to increase the capability of our system in future work to use other imaging techniques, such as CT scans, to provide an integrated system that helps physicians in the detection of COVID-19 using various imaging techniques as well as testing our proposed model by using various datasets from different repositories. Finally, we plan to reduce the trainable parameters of our models to minimize the computational cost.

Author credit statement

1-Conception or design of the work: Mohamed Abdelazim, Eman Abdelhalim, Hagar H. Eldawoudy (35%/35%/30%). 2-Data collection and tools: Mohamed Abdelazim, Eman Abdelhalim, Hagar H. Eldawoudy (30%/30%/40%). 3-Data analysis and interpretation: Mohamed Abdelazim, Eman Abdelhalim, Hagar H. Eldawoudy (30%/40%/30%). 4-Methodology: Mohamed Abdelazim, Eman Abdelhalim, Hagar H. Eldawoudy (40%/35%/25%). 5-Project administration: Mohamed Abdelazim, Eman Abdelhalim, Hagar H. Eldawoudy (40%/30%/30%). 6-Software: Mohamed Abdelazim, Eman Abdelhalim, Hagar H. Eldawoudy (30%/30%/40%). 7-Drafting the article: Mohamed Abdelazim, Eman Abdelhalim, Hagar H. Eldawoudy (30%/30%/40%).

8-Critical revision of the article: Mohamed Abdelazim, Eman Abdelhalim, Hagar H. Eldawoudy (35%/40%/25%). 1- Eng Hagar Hesham Eldawoudy, Teaching Assistant, Electronics and Communications Engineering Department, Faculty of Engineering. (Email: hagerhesham653@gmail.com). 2- Prof. Mohamed Abdelazim, Electronics and Communications Engineering Department, Faculty of Engineering. (Email: mazim12@mans.edu.eg). 3- Asst. Prof. Eman Abdelhalim, Electronics and Communications Engineering Department, Faculty of Engineering. (Email: eman_haleim@mans.edu.eg).

Authored by

Eng. Hagar Hesham Eldawoudy

Teaching Assistant -Dept of Electronics and CommuTeaching Assistant -Dept. of Electronics and Communications Engineering, Faculty of Engineering, Mansoura University.

Supervised by

Prof. Mohamed Abdelazim Mohamed

Professor, Dept. of Electronics and Communications Engineering, Faculty of Engineering, Mansoura University.

Asst. Prof. Eman Abdelhalim

Assistant Professor, Dept. of Electronics and Communications Engineering, Faculty of Engineering, Mansoura University.

Funding statement

There is no funding for the researcher.

Conflicts of interest

There is no conflict of interest.

References

- Abdelhamid, A.A., et al., 2022. Multi-classification of chest X-rays for COVID-19 diagnosis using deep learning algorithms. *Appl. Sci.* 12, 4. <https://doi.org/10.3390/app12042080> issn: 2076-3417. <https://www.mdpi.com/2076-3417/12/4/2080>.
- Abiyev, R.H., Ma'aitah, M.K.S., 2018. Deep convolutional neural networks for chest diseases detection. *J. Healthc. Eng.* <https://doi.org/10.1155/2018/4168538>.
- Ai, T., et al., 2020. Correlation of chest CT and RT-PCR testing for coronavirus disease 2019 (COVID-19) in China: a report of 1014 cases. *Radiology* 296, E32–E40. <https://doi.org/10.1148/radiol.2020200642>. PMID: 32101510.
- Al-Shourbaji, I., et al., 2023. A deep batch normalized convolution approach for improving COVID-19 detection from chest x-ray images. *Pathogens* 12, 1 issn: 2076-0817. <https://www.mdpi.com/2076-0817/12/1/17>.
- Allam, E., Alfonse, M., Salem, A.B.M., 2022. Artificial intelligence techniques for classification of eye tumors: a survey. In: 2022 5th International Conference on Computing and Informatics, pp. 175–179. <https://doi.org/10.1109/ICCI54321.2022.9756067>.
- Alyoubi, W.L., Shalash, W.M., Abulkhair, M.F., 2020. Diabetic retinopathy detection through deep learning techniques: a review. *Inform. Med. Unlock* 20, 100377. <https://doi.org/10.1016/j.imu.2020.100377>. url issn: 2352-9148. <https://www.sciencedirect.com/science/article/pii/S2352914820302069>.
- Amin, J., et al., 2022. Brain tumor detection and classification using machine learning: a comprehensive survey. *Complex Intell. Syst.* 8, 3161–3183. <https://doi.org/10.1007/s40747-021-00563-y>.
- Amrane, M., et al., 2018. Breast cancer classification using machine learning. In: 2018 Electr Electron Comput Sci Biomed Eng Meet, pp. 1–4. <https://doi.org/10.1109/EBBT.2018.8391453>.
- Bhat, R., 2020. Gradient Descent with Momentum. <https://towardsdatascience.com/gradient-descent-with-momentum-59420f626c8f>.
- Cohen, J.P., 2020. Covid-Chestxray-Dataset url: <https://github.com/ieee8023/covid-chestxray-dataset>.
- Cozzi, D., Albanesi, M., Cavigli, E., Moroni, C., Bindi, A., Luvarà, S., Lucarini, S., Busoni, S., Mazzoni, L.N., Miele, V., 2020. Chest X-ray in new Coronavirus Disease 2019 (COVID-19) infection: findings and correlation with clinical outcome. *Radiologia Medica* 125 (8), 730–737. <https://doi.org/10.1007/s11547-020-01232-9>.
- Das, A.K., et al., 2021. Automatic COVID-19 detection from X-ray images using ensemble learning with convolutional neural network. *Pattern Anal. Appl.* 24, 1111–1124. <https://doi.org/10.1007/s10044-021-00970-4>.
- Deng, J., et al., 2009. ImageNet: a large-scale hierarchical image database. In: IEEE Conference on Computer Vision and Pattern Recognition, pp. 248–255. <https://doi.org/10.1109/CVPR.2009.5206848>.
- Gupta, A., 2018. Introduction to Deep Learning: Part 1 url: <https://medium.com/analytics-vidhya/a-complete-guide-to-adam-and-rmsprop-optimizer-75f4502d83be>.
- He, K., et al., 2016. Deep residual learning for image recognition. In: 2016 IEEE Conference on Computer Vision and Pattern Recognition (CVPR), pp. 770–778. <https://doi.org/10.1109/CVPR.2016.90>.
- Huang, G., et al., 2018. Densely connected convolutional networks. In: 2017 IEEE Conference on Computer Vision and Pattern Recognition (CVPR), pp. 2261–2269. <https://doi.org/10.1109/CVPR.2017.243>.
- Ibrahim, D.M., Elshennawy, N.M., Sarhan, A.M., 2021. Deep-chest: multi-classification deep learning model for diagnosing COVID-19, pneumonia, and lung cancer chest diseases. *Comput. Biol. Med.* 132, 104348. <https://doi.org/10.1016/j.compbiomed.2021.104348>. url issn: 0010-4825. <https://www.sciencedirect.com/science/article/pii/S0010482521001426>.
- Kadampur, M.A., Al Riyae, S., 2020. Skin cancer detection: applying a deep learning based model driven architecture in the cloud for classifying dermal cell images. *Inform. Med. Unlock* 18, 100282. <https://doi.org/10.1016/j.imu.2019.100282> issn: 2352-9148. <https://www.sciencedirect.com/science/article/pii/S2352914819302047>.
- Khandelwal, R., 2019. Overview of Different Optimizers for Neural Networks. <https://medium.datadriveninvestor.com/overview-of-different-optimizers-for-neural-networks-e0ed119440c3>.
- Kini, A.S., et al., 2022. Ensemble deep learning and internet of things-based automated COVID-19 diagnosis framework. *Cont. Media Mol. Imag.* 10. <https://doi.org/10.1155/2022/7377502>.
- Kumar, N., et al., 2023. Novel deep transfer learning model for COVID-19 patient detection using X-ray chest images. *Ambient Intell. Hum. Comput.* 14, 469–478. <https://doi.org/10.1007/s12652-021-03306-6>.
- Kundu, R., et al., 2021. COVID-19 detection from lung CT-Scans using a fuzzy integral-based CNN ensemble. *Comput. Biol. Med.* 138, 104895. <https://doi.org/10.1016/j.compbiomed.2021>.

104895. url issn: 0010-4825. <https://www.sciencedirect.com/science/article/pii/S0010482521006892>.
- Li, Y., Xia, L., 2020. Coronavirus disease 2019 (covid-19): role of chest ct in diagnosis and management. *Am. J. Roentgenol.* 214, 1280–1286. <https://doi.org/10.2214/ajr.20.22954>.
- Long, C.-Q., Xu, H., Shen, Q., Li, H., 2020. Diagnosis of the Coronavirus disease (COVID-19): rRT-PCR or CT? *Eur. J. Radiol.* 126, 108961. <https://doi.org/10.1016/j.ejrad.2020.108961>.
- Mahanty, C., Kumar, R., Patro, S.G.K., 2022. Internet of Medical Things-Based COVID-19 detection in CT images fused with fuzzy ensemble and transfer learning models. *New Generat. Comput.* 40, 1125–1141. <https://doi.org/10.1007/s00354-022-00176-0>.
- Mayanglambam, G., 2020. Deep Learning Optimizers. <https://towardsdatascience.com/deep-learning-optimizers-436171c9e23f>.
- Mooney, P., 2018. Chest X-Ray Images (Pneumonia). <https://www.kaggle.com/datasets/paultimothymooney/chest-xray-pneumonia>.
- Musstafa, 2021. Optimizers in Deep Learning. <https://medium.com/mllearning-ai/optimizers-in-deep-learning-7bf81fed78a0>.
- Narin, A., Kaya, C., Pamuk, Z., 2021. Automatic detection of Coronavirus disease (COVID-19) using X-ray images and deep convolutional neural networks. *Pattern Anal. Appl.* 24, 1207–1220. <https://doi.org/10.1007/s10044-021-00984-y>.
- Nayak, S.R., et al., 2023. An efficient deep learning method for detection of COVID-19 infection using chest x-ray images. *Diagnostics* 13. <https://doi.org/10.3390/diagnostics13010131>.
- Oppermann, A., 2023. Optimization in Deep Learning: AdaGrad, RMSProp, ADAM. <https://artemoppermann.com/optimization-in-deep-learning-adagrad-rmsprop-adam/>.
- Rahman, T., 2020. COVID-19 Radiography Database. <https://www.kaggle.com/datasets/tawsifurrahman/covid19-radiography-database>.
- Raikote, P., 2020. Covid-19 Image Dataset url: <https://www.kaggle.com/pranavraikokte/covid19-image-dataset>.
- Rodge, D., 2021. A Gentle Introduction to Ensemble Learning. <https://medium.com/@deeproodge/a-gentle-introduction-to-ensemble-learning-fc00fc33f97f>.
- Roy, P.K., Kumar, A., 2022. Early prediction of COVID-19 using ensemble of transfer learning. *Comput. Electr. Eng.* 101, 108018. <https://doi.org/10.1016/j.compeleceng.2022.108018> issn: 0045-7906. <https://www.sciencedirect.com/science/article/pii/S004579062200283X>.
- Saha, P., Sadi, M.S., Islam, Md.M., 2021. EMCNet: automated COVID-19 diagnosis from X-ray images using convolutional neural network and ensemble of machine learning classifiers. *Inform. Med. Unlock.* 22, 100505. <https://doi.org/10.1016/j.imu.2020.100505>.
- Sanghvirajit, 2021. A Complete Guide to Adam and RMSprop Optimizer. <https://medium.com/analytics-vidhya/a-complete-guide-to-adam-and-rmsprop-optimizer-75f4502d83be>.
- Sethy, P., Behera, S., 2020. Detection of coronavirus disease (COVID-19) based on deep features. Preprints. <https://doi.org/10.20944/preprints202003.0300.v1>.
- Shyni, H., Chitra, E., 2022. A comparative study of X-ray and CT images in COVID-19 detection using image processing and deep learning techniques. *Comput. Meth. Prog. Biomed. Update* 2, 100054. <https://doi.org/10.1016/j.cmpbup.2022.100054>.
- Simonyan, K., Zisserman, A., 2015. Very deep convolutional networks for large-scale image recognition. In: 3rd International Conference on Learning Representations (ICLR 2015), pp. 1–14. <https://doi.org/10.48550/arXiv.1409.1556> arXiv: 1409.1556.
- Solaiman, I., Sanjana, T., 2022. X-ray classification to detect COVID-19 using ensemble model Proceedings of the 14th International Conference on Agents and Artificial Intelligence 2, pp. 375–386. <https://doi.org/10.5220/0010847200003116>.
- Srivastava, N., 2022. Optimizers Supported by the PyTorch Framework. In-depth guide: <https://www.e2enetworks.com/blog/optimizers-supported-by-the-pytorch-framework-in-depth-guide>.
- Srivastava, G., et al., 2022. CoviXNet: a novel and efficient deep learning model for detection of COVID-19 using chest X-Ray images. *Biomed. Signal Proc. Contr.* 78, 103848. <https://doi.org/10.1016/j.bspc.2022.103848>.
- Vidyalaya, R., 2020. Performance Metrics for Classification Machine Learning Problems. <https://towardsdatascience.com/performance-metrics-for-classification-machine-learning-problems-97e774a007>.
- Yamashita, R., et al., 2018. Convolutional neural networks: an overview and application in radiology. *Insights Imag.* 9, 611–629. <https://doi.org/10.1007/s13244-018-0639-9>.
- Zhou, T., et al., 2021. The ensemble deep learning model for novel COVID-19 on CT images. *Appl. Soft Comput.* 98, 106885. <https://doi.org/10.1016/j.asoc.2020.106885> issn: 1568-4946. <https://www.sciencedirect.com/science/article/pii/S1568494620308231>.